

# A 2.4–12 $\mu\text{m}$ spectrophotometric study with ISO of Cygnus X-3 in quiescence<sup>★</sup>

L. Koch-Miramond<sup>1</sup>, P. Ábrahám<sup>2,3</sup>, Y. Fuchs<sup>1,4</sup>, J.-M. Bonnet-Bidaud<sup>1</sup>, and A. Claret<sup>1</sup>

<sup>1</sup> DAPNIA/Service d'Astrophysique, CEA-Saclay, 91191 Gif-sur-Yvette Cedex, France

<sup>2</sup> Konkoly Observatory, PO Box 67, 1525 Budapest, Hungary

<sup>3</sup> Max-Planck-Institut für Astronomie, Königstuhl 17, 69117 Heidelberg, Germany

<sup>4</sup> Université Paris VII, France

Received 5 June 2002 / Accepted 28 June 2002

**Abstract.** We present mid-infrared spectrophotometric results obtained with the ISO on the peculiar X-ray binary Cygnus X-3 in quiescence, at orbital phases 0.83 to 1.04. The 2.4–12  $\mu\text{m}$  continuum radiation observed with ISOPHOT-S can be explained by thermal free-free emission in an expanding wind with, above 6.5  $\mu\text{m}$ , a possible additional black-body component with temperature  $T \sim 250$  K and radius  $R \sim 5000 R_{\odot}$  at 10 kpc, likely due to thermal emission by circumstellar dust. The observed brightness and continuum spectrum closely match that of the Wolf-Rayet star WR 147, a WN8+B0.5 binary system, when rescaled at the same 10 kpc distance as Cygnus X-3. A rough mass loss estimate assuming a WN wind gives  $\sim 1.2 \times 10^{-4} M_{\odot} \text{yr}^{-1}$ . A line at  $\sim 4.3 \mu\text{m}$  with a more than  $4.3 \sigma$  detection level, and with a dereddened flux of 126 mJy, is interpreted as the expected He I 3p–3s line at 4.295  $\mu\text{m}$ , a prominent line in the WR 147 spectrum. These results are consistent with a Wolf-Rayet-like companion to the compact object in Cyg X-3 of WN8 type, a later type than suggested by earlier works.

**Key words.** stars: binaries: close – stars: individual: Cyg X-3 – stars: Wolf-Rayet – stars: mass-loss – infrared: stars

## 1. Introduction

Cygnus X-3 has been known as a binary system since its discovery by Giacconi et al. (1967), but there is still debate about the masses of the two stars and the morphology of the system (for a review see Bonnet-Bidaud & Chardin 1988). The distance of the object is 8–12.5 kpc with an absorption on the line of sight  $A_V \sim 20$  mag (van Kerkwijk et al. 1996). The flux modulation at a period of 4.8 hours, first discovered in X-rays (Parsignault 1972), then at near infrared wavelengths (Becklin et al. 1973), and observed simultaneously at X-ray and near-IR wavelengths by Mason et al. (1986), is believed to be the orbital period of the binary system. Following infrared spectroscopic measurements (van Kerkwijk et al. 1992), where WR-like features have been detected in *I* and *K* band spectra, the nature of the mass-donating star is suggested to be a Wolf-Rayet-like star, but an unambiguous classification, similar to the other WR stars, is still lacking. Mitra (1996) and Vanbeveren et al. (1998) pointed out that it is not possible to find a model that meets all the observed properties of

Cygnus X-3 where the companion star is a normal Population I Wolf-Rayet star with a spherically symmetric stellar wind. In the evolution model originally proposed by van den Heuvel & de Loore (1973) a final period of the order of 4.8 h may result from a system with initial masses  $M_1^0 = 15 M_{\odot}$ ,  $M_2^0 = 1 M_{\odot}$ ,  $P^0 = 5$  d, the final system being a neutron star accreting at a limited rate of  $\sim 10^{-7} M_{\odot} \text{yr}^{-1}$ , from the wind of a core He burning star of about  $3.8 M_{\odot}$ . Vanbeveren et al. (1998) proposed that the progenitor of Cygnus X-3 is a  $50 M_{\odot} + 10 M_{\odot}$  system with  $P^0 = 6$  d; after spiral-in of the black hole into the envelope of the companion, the hydrogen reach layers are removed, and a 2–2.5  $M_{\odot}$  Wolf-Rayet like star remains with  $P = 0.2$  d. A system containing a black hole and an He core burning star is also favored by Ergma & van den Heuvel (1998). In addition, Cygnus X-3 undergoes giant radio bursts and there is evidence of jet-like structures moving away from Cygnus X-3 at 0.3–0.9 c (Mioduszewski et al. 1998; 2001; Martí et al. 2001).

The main objective of the Infrared Space Observatory (ISO) spectrophotometric measurements in the 2.4–12  $\mu\text{m}$  range was to constrain further the nature of the companion star to the compact object: the expected strong He lines as well as the metallic lines in different ionization states are important clues, together with the spectral shape of the continuum in a wavelength range as large as possible. An additional motivation for the imaging photometry with ISOCAM was to provide

Send offprint requests to: L. Koch-Miramond,  
e-mail: lkoch@discovery.saclay.cea.fr

<sup>★</sup> Based on observations with ISO, an ESA project with instruments funded by ESA Member States (especially the PI countries: France, Germany, The Netherlands and the UK) and with the participation of ISAS and NASA.

**Table 1.** The ISO observing modes, ISO identifications, wavelength ranges and observing times on April 7, 1996, used on Cygnus X-3.

Instrument	TDNUM	Wavelength range ( $\mu\text{m}$ )	Aperture arcsec	Total observing time (s)	TU (start)
ISOCAM-LW10	14200701	8–15	1.5	1134	6:57:09
ISOPHOT-SS	14200803	2.4–4.9	24 × 24	4096	7:16:47
ISOPHOT-SL		5.9–11.7	24 × 24		
ISOPHOT-P 3.6	14200802	2.9–4.1	10	1100	8:27:33
ISOPHOT-P 10		9–10.9	23		
ISOPHOT-P 25		20–29	52		
ISOPHOT-P 60		48–73	99		

spatial resolution to a possible extended emission feature as a remnant of the expected high mass loss from the system. The paper is laid out as follows. In Sect. 2 observational aspects are reviewed. Section 3 summarizes the results on the continuum and line emissions from Cygnus X-3 and four Wolf-Rayet stars of WN 6, 7 and 8 types, and reviews the constraints set by the present observations on the wind and on the nature of the companion to the compact object in Cygnus X-3. Finally, Sect. 4 summarizes the conclusions of this paper.

## 2. Observations and data reduction

We observed Cygnus X-3 with the Infrared Space Observatory (ISO, see Kessler et al. 1996) on April 7, 1996 corresponding to JD 2 450 180.8033 to 2 450 180.8519. The subsequent observing modes were: ISOCAM imaging photometry at 11.5  $\mu\text{m}$  (LW10 filter, bandwidth 8 to 15  $\mu\text{m}$ ), ISOPHOT-S spectrophotometry in the range 2.4–12  $\mu\text{m}$ , for 4096 s, covering the orbital phases 0.83 to 1.04 (according to the parabolic ephemeris of Kitamoto et al. 1992); ISOPHOT multi-filter photometry at central wavelengths 3.6, 10, 25 and 60  $\mu\text{m}$ . Observing modes and observation times are summarized in Table 1. Preliminary results were presented in Koch-Miramond et al. (2001).

### 2.1. ISOPHOT-S data reduction

A low resolution mid-infrared spectrum of Cygnus X-3 was obtained with the ISOPHOT-S sub-instrument. The spectrum covered the 2.4–4.9 and 5.9–11.7  $\mu\text{m}$  wavelength ranges simultaneously with a spectral resolution of about 0.04 and 0.1  $\mu\text{m}$ , respectively. The observation was performed in the triangular chopped mode with two background positions located at  $\pm 120''$ , and with a dwelling time of 128 s per chopper position. The field of view is  $24'' \times 24''$ . The whole measurement consisted of 8 OFF1–ON–OFF2–ON cycles and lasted 4096 s.

The ISOPHOT-S data were reduced in three steps. We first used the Phot Interactive Analysis (PIA<sup>1</sup>, Gabriel et al. 1997) software (version 8.2) to filter out cosmic glitches in the raw data and to determine signals by performing linear fits to the integration ramps. After a second deglitching step, performed on the signals, a dark current value appropriate to the satellite

orbital position of the individual signal was subtracted. Finally we averaged all non-discarded (typically 3) signals in order to derive a signal per chopper step. Due to detector transient effects, at the beginning of the observation the derived signals were systematically lower than those in the consolidated part of the measurement. We then discarded the first  $\sim 800$  s (3 OFF–ON transitions), and determined an average [ON–OFF] signal for the whole measurement by applying a 1-dimensional Fast Fourier Transformation algorithm (for the application of FFT methods for ISOPHOT data reduction see Haas et al. 2000). The [ON–OFF] difference signals were finally calibrated by applying a signal-dependent spectral response function dedicated to chopped ISOPHOT-S observations (Acosta-Pulido & Ábrahám 2001), also implemented in PIA.

In order to verify our data reduction scheme (which is not completely standard due to the application of the FFT algorithm) and to estimate the level of calibration uncertainties, we reduced HD 184400, an ISOPHOT standard star observed in a similar way as Cygnus X-3. The results were very consistent with the model prediction of the star, and we estimate that the systematic uncertainty of our calibration is less than 10%.

### 2.2. ISOPHOT spectral energy distribution

The observed spectral energy distribution is shown in Fig. 1. The observed (not dereddened) continuum flux in the range 2.4–7  $\mu\text{m}$  is  $20 \pm 10$  mJy in good agreement with that observed by Ogle et al. (2001) with ISOCAM on the same day (the dereddened fluxes are shown in Fig. 2); the observed flux decreases to about  $10 \pm 8$  mJy around 9  $\mu\text{m}$ .

An unresolved line is observed at about 4.3  $\mu\text{m}$  peaking at  $57 \pm 10$  mJy. The linewidth is 0.04  $\mu\text{m}$ , consistent with the instrumental response and corresponding to  $\sim 2500$  km s<sup>-1</sup>. Note that the measured line flux might be underestimated because the ISOPHOT-S pixels are separated by small gaps, and a narrow line might fall into a gap.

### 2.3. ISOPHOT-P data analysis and results

The data reduction in the multi-filter mode was performed using the Phot Interactive Analysis (Gabriel et al. 1997) software. After corrections for non-linearities of the integration ramps, the signal was transformed to a standard reset interval. Then an orbital dependent dark current was subtracted and cosmic

<sup>1</sup> PIA is a joint development by the ESA Astrophysics Division and the ISOPHOT consortium led by the Max-Planck-Institut für Astronomie, Heidelberg.

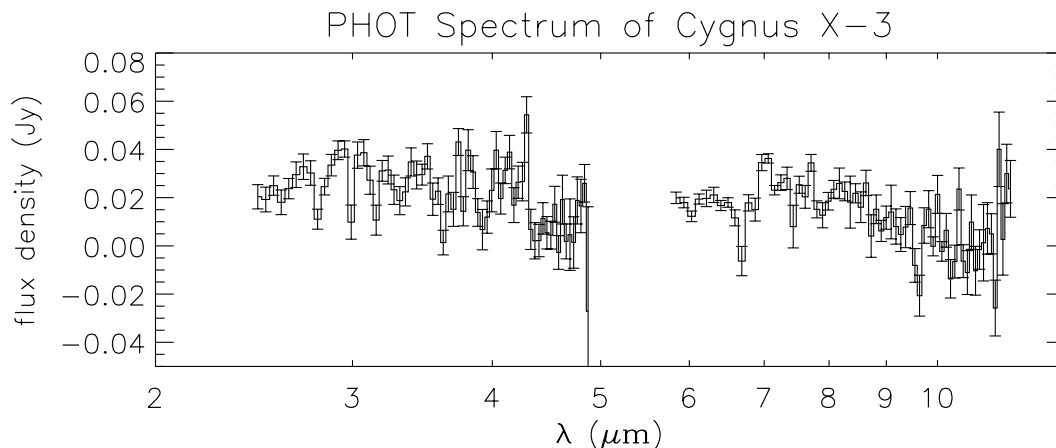


**Fig. 1.** Observed spectrum of Cygnus X-3 in the 2.4–12  $\mu\text{m}$  range, obtained with the FFT method.

ray hits were removed. In case the signal did not fully stabilize during the measurement time due to the detector transients, only the last part of the data stream was used. The derived flux densities were corrected for the finite size of the aperture by using the standard correction values as stated in the ISOPHOT Observer’s Manual (Klaas et al. 1994). The flux detected at 3.6  $\mu\text{m}$  (bandwidth 1  $\mu\text{m}$ ) in the 10'' diameter aperture is  $8.1 \pm 3.3$  mJy at a confidence level of  $2.4\sigma$ . No detection above the galactic noise was obtained at 10, 25 and 60  $\mu\text{m}$  with 23'', 52'' and 99'' diameter aperture, respectively.

#### 2.4. ISOCAM data reduction and results

The LW10 filter centered at 11.5  $\mu\text{m}$  was used with the highest spatial resolution of  $1.5'' \times 1.5''$  per pixel. The ISOCAM data were reduced with the Cam Interactive Analysis software (CIA<sup>2</sup>) version 3.0, following the standard processing outlined in Starck et al. (1999). First a dark correction was applied, then a de-glitching to remove cosmic ray hits, followed by a transient correction to take into account memory effects, using the inversion algorithm of Abergel et al. (1996), and a flat-field correction. Then individual images were combined into the final raster map, whose pixel values were converted into milli-Jansky flux densities. No colour correction was applied. A point source is clearly visible at the Cygnus X-3 position on the ISOCAM map at 11.5  $\mu\text{m}$ . The measured flux is  $7.0 \pm 2.0$  mJy above a uniform background at a level of about 1.2 mJy, in good agreement with our ISOPHOT result. This flux is lower than the  $15.2 \pm 1.6$  mJy (at 11.5  $\mu\text{m}$ ) measured by Ogley et al. (2001), on the same day, using ISOCAM/LW10 with a  $6'' \times 6''$  aperture.

The high resolution configuration of the ISOCAM camera has been used to constrain the spatial extension of the infrared source. The measured *FWHM* for the source is  $3.90 \pm 0.45$  arcsec (mean value of the four individual images composing the final raster map). This can be compared to the ISOCAM

catalogued point spread functions at these energy and configuration which show a *FWHM* mean value of  $3.44 \pm 0.45$  arcsec, including the effects of the satellite jitter and of the pixel sampling. The slightly larger value for Cygnus X-3, though only marginally significant, might therefore indicate an extended source. The deconvolved extension would be  $1.84 \pm 0.64$  arcsec which at a distance of 10 kpc corresponds to a linear extension of  $\sim 2.7 \times 10^{17}$  cm. The extended infrared source may be the result of the heating of the surrounding medium by the radio jets whose existence have been now clearly demonstrated both at arcsec (Martí et al. 2000, 2001) and sub-arcsec (Mioduszewski et al. 2001) scales, but it clearly deserves confirmation.

### 3. Results and discussion

#### 3.1. Continuum spectral energy distribution: Model fitting and comparison with four Wolf-Rayet stars

The dereddening of the Cygnus X-3 spectrum is made using either Lutz et al. (1996) or Draine (1989) laws, and using an absorption value of  $A_V = 20$  mag (van Kerkwijk et al. 1996); the two dereddened spectra are shown in Fig. 2. They have clearly different shapes, but since the molecular composition of the absorbing material on the line of sight to Cygnus X-3 is unknown, we cannot choose between these two laws.

The spectral fitting of the dereddened spectra is shown in Fig. 3 and the results are given in Table 2. With the Lutz et al. (1996) law the best fit is obtained with a unique power law  $S_\nu \propto \lambda^{-0.6 \pm 0.3}_{0.4}$  with a reduced  $\chi^2 = 4.3$  in the 2.4–12  $\mu\text{m}$  range, in good agreement with the Ogley et al (2001) result. With the Draine (1989) law the best fit is obtained with the sum of two components: a power law with slope  $\lambda^{-1.6 \pm 0.2}$  and a black body at  $T = 250$  K with a radius of 5000  $R_\odot$  at a distance of 10 kpc, (reduced  $\chi^2 = 4.2$  between 2.4 and 12  $\mu\text{m}$ ), a hint of the presence of circumstellar dust. The power law part of the continuum spectrum ( $S_\nu \propto \lambda^{-\alpha}$ ) can be explained by free-free emission of an expanding wind in the intermediate case between optically thick ( $\alpha = 2$ ) and optically thin ( $\alpha \sim 0$ ) regimes (Wright & Barlow 1975).

Using the ISO archive data we have analysed the SWS spectra of four Wolf-Rayet stars: WR 147 (WN8+B0.5),

<sup>2</sup> CIA is a joint development by the ESA Astrophysics Division and the ISOCAM consortium. The ISOCAM consortium was led by the ISOCAM PI, C. Cesarsky, Direction des Sciences de la Matière, C.E.A, France.

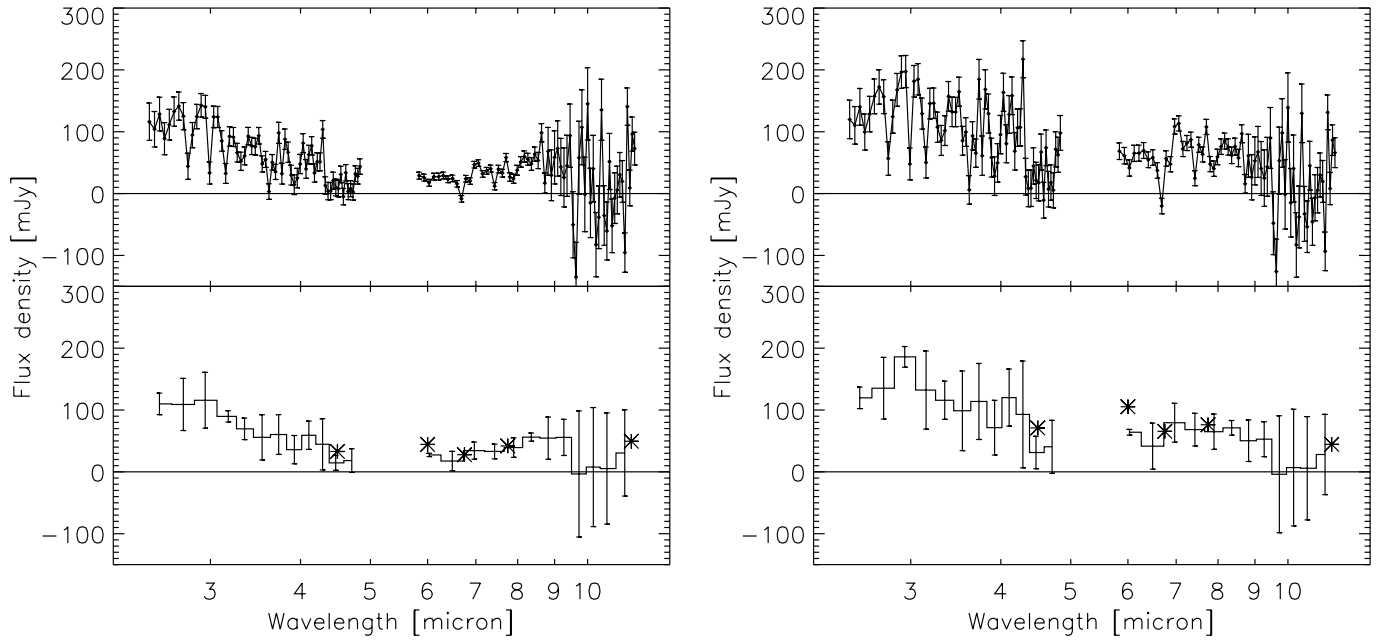


**Fig. 2.** Dereddened spectrum of Cygnus X-3 using either Draine (1989) law (left) or Lutz et al. (1996) law (right). The asterisks (\*) in the lower panel represent the Ogley et al. (2001) ISOCAM results, after dereddening by Draine (1989) (left) and Lutz (right).

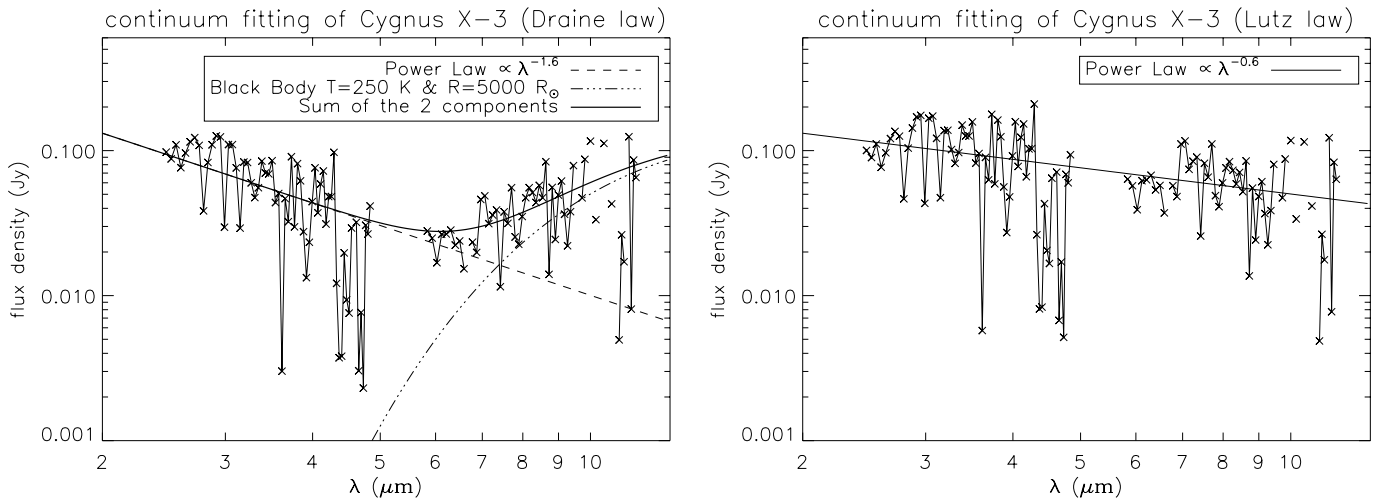


**Fig. 3.** Best fitting of the two dereddened spectra of Cygnus X-3 shown in Fig. 2.

WR 136 (WN6b), WR 134 (WN6) and WR 78 (WN7) whose main characteristics are given in Table 3. We compare them to the Cygnus X-3 spectrum, after smoothing the SWS spectra to the resolution of the ISOPHOT-S instrument (using an IDL routine of B. Schulz downloaded from the Home Page of the ISO Data Centre at Vilspa). The observed WR spectra are shown in Fig. 4 on top of the observed Cygnus X-3 spectrum; the identification of the emission lines is from Morris et al. (2000).

The dereddened spectra of the Wolf-Rayet stars, using either the Draine (1989) law or the Lutz et al. (1996) law with the  $A_V$  shown in Table 3, have been fitted with power law slopes given in Table 2. Wolf-Rayet stars emit free-free continuum radiation from their extended ionized stellar wind envelopes and the different slopes reflect different conditions in the wind (Williams et al. 1997). It is noticeable that the mean continuum flux density of Cygnus X-3 is the same (within a

**Table 2.** Comparison of the infrared continuum spectra of Cygnus X-3 and four WR stars: power law slopes  $\alpha$  such as  $S_\nu \propto \lambda^{-\alpha}$  and  $4.7 \mu\text{m}$  flux densities rescaled at 10 kpc.

Object	PL slope <sup>a</sup>	PL slope <sup>b</sup>	Flux at $4.7\mu\text{m}$ (Jy)
Cygnus X-3	$1.6 \pm 0.2^c$	$0.6 \pm_{0.4}^{0.3}$	$0.079 \pm 0.011$
WR 78	$1.4 \pm 0.2^d$	$1.4 \pm 0.2$	$0.114 \pm 0.008$
WR 134	$0.2 \pm 0.2^d$	$0.2 \pm 0.2$	$0.081 \pm 0.006$
WR 136	$1.0 \pm 0.2^e$	$1.0 \pm 0.2$	$0.076 \pm 0.006$
WR 147	$1.6 \pm 0.1^c$	$1.0 \pm 0.1$	$0.085 \pm 0.005$

<sup>a</sup> Dereddening with Draine (1989) law.

<sup>b</sup> Dereddening with Lutz et al. (1996) law; fit between  $2.4\text{--}12 \mu\text{m}$ .

<sup>c</sup> Fit between  $2.4\text{--}6.5 \mu\text{m}$ .

<sup>d</sup> Fit between  $2.4\text{--}12 \mu\text{m}$ .

<sup>e</sup> Fit between  $2.4\text{--}8 \mu\text{m}$ .

**Table 3.** The four Wolf-Rayet stars observed with ISO/SWS.

Star	Type	Binarity	Distance	$A_V^a$	Reference	TDTNUM
WR 78	WN7h <sup>a</sup> WNL	No	2.0 kpc	1.48–1.87	Crowther et al. (1995a)	45800705
WR 134	WN6	possible	~2.1 kpc	1.22–1.99	Morel et al. (1999)	17601108
WR 136	WN6b(h) WNE-s <sup>b</sup>	possible	1.8 kpc	1.35–2.25	Stevens & Howarth (1999)	38102211
WR 147	WN8(h) WNL	B0.5V at 0.554''	630 ± 70 pc	11.2	Morris et al. (1999, 2000)	33800415

<sup>a</sup> From van der Hucht (2001) except for WR 147.

<sup>b</sup> From Crowther et al. (1995b).

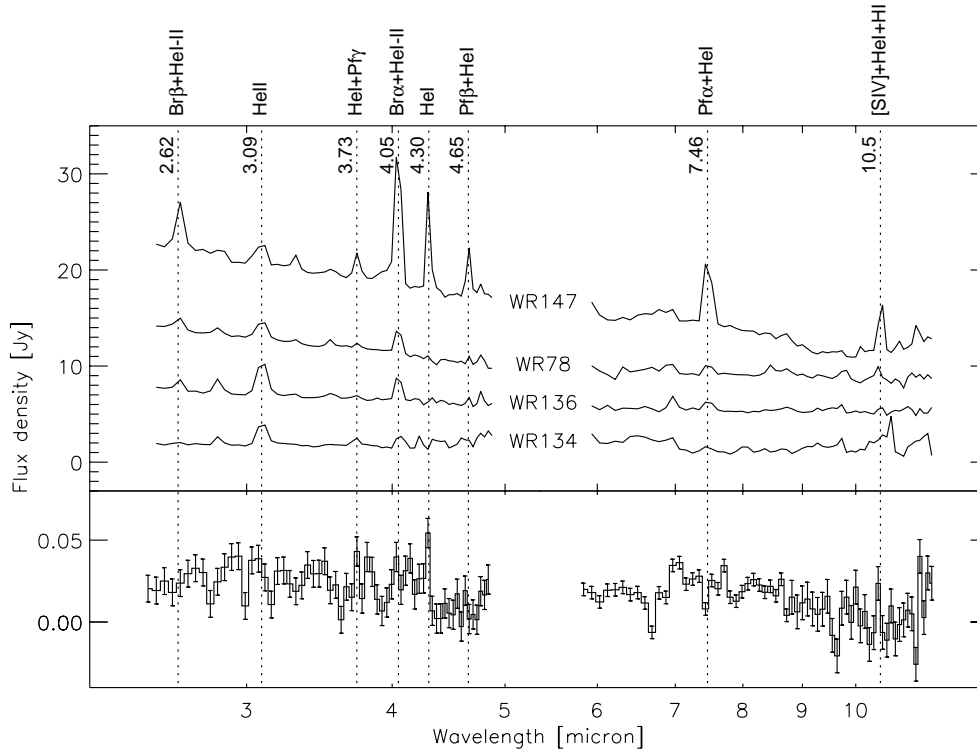


**Fig. 4.** Observed spectra of Cygnus X-3 and four Wolf-Rayet stars (not dereddened). An arbitrary vertical offset has been added to the WR spectra for clarity. The identification of the emission lines is from Morris et al. (2000).

factor 1.5 at 4.7  $\mu\text{m}$  as seen in Table 2) as that of the four WR stars when their flux density is rescaled to a Cygnus X-3 distance of 10 kpc.

The comparison between the Cygnus X-3 spectrum and that of the Wolf-Rayet WR 147 at 10 kpc is shown in Fig. 5 after dereddening with the Draine (1989) law (left) and with the Lutz et al. (1996) law (right). The WR 147 spectrum appears as the closest WR one to the Cygnus X-3 spectrum, with almost the same mean flux density at 10 kpc and the same power law slope (within the statistical errors).

We note that WR 147 is known as a colliding-wind binary that has been spatially resolved (Williams et al. 1997; Skinner et al. 1999), with a separation on the sky large enough for the wind-wind collision zone between the stars to be resolved at near-infrared and radio (Williams et al. 1997), and X-ray energies (Pittard et al. 2002). The spectral energy distribution of WR 147 in the 0.5  $\mu\text{m}$  to 2 mm wavelength range (including all components) shown by Williams et al. (1997) is dominated by the free-free emission from the stellar wind of the WN8 star;

in the 2 to 10  $\mu\text{m}$  range these authors find  $\alpha = 1.0$ , in good agreement with our ISOPHOT-S measurement (when dereddened with the Lutz et al. 1996 law); and in the mid-infrared to radio range they find  $\alpha = 0.66$ .

### 3.2. Emission lines; comparison with four Wolf-Rayet stars

The measured 4.3  $\mu\text{m}$  line flux above the continuum in the Cygnus X-3 spectrum is  $58 \pm 11$  mJy (dereddening with the Draine 1989 law), and  $126 \pm 25$  mJy (dereddening with the Lutz et al. 1996 law), using respectively  $\alpha = 1.6$  and  $\alpha = 0.6$ , the best fitted continuum slopes as given in Table 3, both detections being at more than  $4.3\sigma$ . This line is interpreted as the HeI (3p-3s) line at 4.295  $\mu\text{m}$ , a prominent line in the WR 147 (WN8+B0.5) spectrum as seen in Morris et al. (2000) and in Fig. 4. Again WR 147 appears as the closest WR to Cygnus X-3 as being the only WR in our sample with a HeI emission line at 4.3  $\mu\text{m}$ , the only line clearly seen in our Cygnus X-3 data.

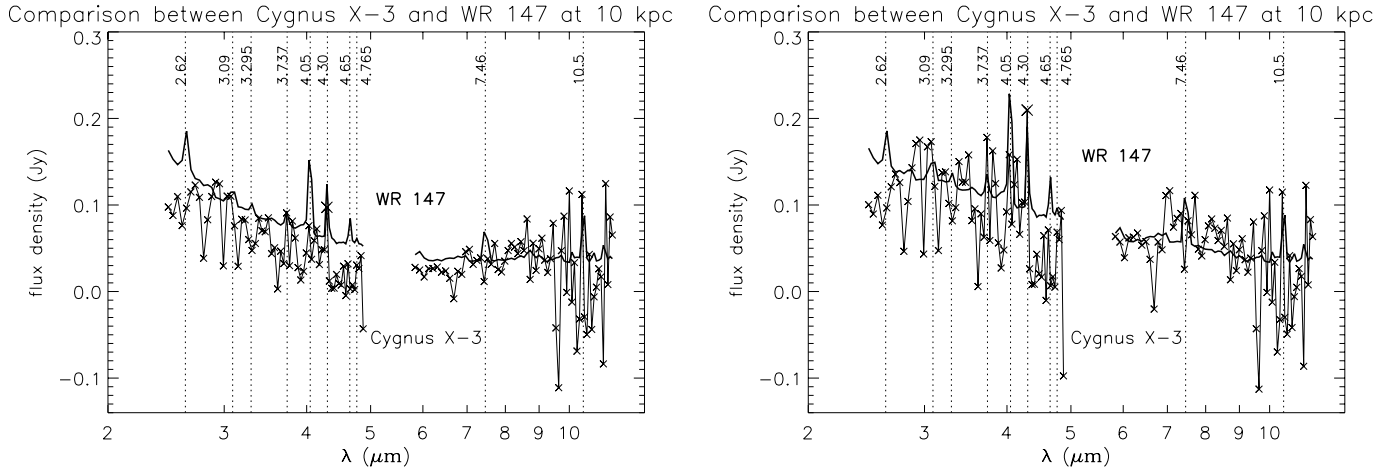


**Fig. 5.** Comparison between the spectral energy distribution of Cygnus X-3 and the one of WR 147 when rescaled at 10 kpc: both dereddened with Draine (1989) law (left) and the Lutz et al. (1996) law (right).

The other expected He lines at 2.62, 3.73, 4.05, 7.46 and 10.5  $\mu\text{m}$  are not detected, probably due to the faintness of the object, at the limits of the instrument's sensitivity. We note (Fig. 4) that the second highest peak in the SS-part of the Cyg X-3 spectrum is at 3.73  $\mu\text{m}$ , and there are also local maxima at 4.05 and 10.5  $\mu\text{m}$ . These expected lines are all blended with H lines and the absence of H observed by van Kerkwijk et al. (1996) in the *I* and *K* band spectra of Cygnus X-3 could explain the weakness or absence of these lines in our data.

We note that the Br $\alpha$ +HeI-II line at 4.05  $\mu\text{m}$  is not detected in Cygnus X-3 in quiescence, but is present in the four Wolf-Rayet stars. Strong HeI and HeII lines have been previously observed in the K-range in Cygnus X-3 during quiescence (van Kerkwijk et al. 1992; 1996, Fender et al. 1999). These lines have been interpreted (van Kerkwijk et al. 1996; Cherepashchuk & Moffat 1994), as emission from the wind of a massive companion star to the compact object, and Fender et al. (1999) suggest that the best candidate is probably an early WN Wolf-Rayet star. We note that the close match we have found between the mid-infrared luminosity and the spectral energy distribution, the HeI emission line in Cygnus X-3 in quiescence, and that of the WR 147, is consistent with a Wolf-Rayet like companion of WN8 type to the compact object in Cygnus X-3, a later type than suggested by earlier works (van Kerkwijk et al. 1996; Fender et al. 1999; Hanson et al. 2000).

### 3.3. Mass loss rate evaluation

As Ogle et al. (2001), we evaluated the mass loss rate of this free-free emitting wind, following the Wright & Barlow (1975) formula (8) giving the emitted flux density (in Jansky) by a stellar wind assumed to be spherical, homogeneous and at a constant velocity:

$$S_\nu = 23.2 \left( \frac{\dot{M}}{\mu v_\infty} \right)^{4/3} \frac{v^{2/3}}{D_{\text{kpc}}^2} \gamma^{2/3} g^{2/3} Z^{4/3} \text{ Jy}$$

where  $D$  is the distance to the source in kpc. It gives:

$$\dot{M} = 5.35 \times 10^{-7} S_\nu^{3/4} (v_{\text{GHz}} \gamma Z^2)^{-1/2} \mu v_\infty M_\odot \times \text{yr}^{-1}$$

(where  $\nu$  is in GHz). With an assumed distance  $D = 10$  kpc, a Gaunt factor  $g = 1$ , a flux density deduced from the continuum fitting (Lutz et al. 1996 law, Fig. 3) of  $S_\nu = 63$  mJy at 6.75  $\mu\text{m}$  ( $4.44 \times 10^4$  GHz), and for a WN-type wind (where the mean atomic weight per nucleon  $\mu = 1.5$ , the number of free electrons per nucleon  $\gamma_e = 1$  and the mean ionic charge  $Z = 1$ ), and with a velocity of  $v_\infty = 1500$  km s $^{-1}$  (van Kerkwijk 1996), one obtains  $\dot{M} = 1.2 \times 10^{-4} M_\odot \text{yr}^{-1}$ . This is in agreement with the mass transfer rate estimated by van Kerkwijk et al. (1996) and (within a factor of 2) by Ogle et al. (2001). This result is in good agreement with the recent revised WN mass-loss rate estimates, which have been lowered by a factor of 2 or 3 due to clumping in the wind (Morris et al. 1999). Note that if we assume a flattened disc-like wind as reported by Fender et al. (1999), who detected double peaked emission lines, the mass loss rate decreases but remains within less than a factor of 2 of that obtained in the spherical case, in all but extreme cases when the ratio of structural length scales exceeds about 10, as shown by Schmid-Burgk (1982). It is noticeable that Churchwell et al. (1992), considering the radio flux from the southern, stellar wind component of WR 147, derived a mass-loss rate of  $\dot{M} = 4.2 \times 10^{-5} M_\odot \text{yr}^{-1}$  and Williams et al. (1997) found a non spherically symmetric stellar wind with a mass-loss rate of  $\dot{M} = 4.6 \times 10^{-5} M_\odot \text{yr}^{-1}$ .

### 3.4. Orbital modulation

Since the length of this spectrophotometric measurement was comparable to the 4.8 h modulation period seen in the *K*-band at the level of 5% (Fender et al. 1995), we attempted to detect this modulation in our data set. The points in Fig. 6 refer to the average for the whole (2–12  $\mu\text{m}$ ) spectrum. Although, as shown in Fig. 6, the measurement uncertainty of the orbitally phase-resolved spectra was relatively high, the data clearly exclude periodic variations of amplitude higher than 15%.

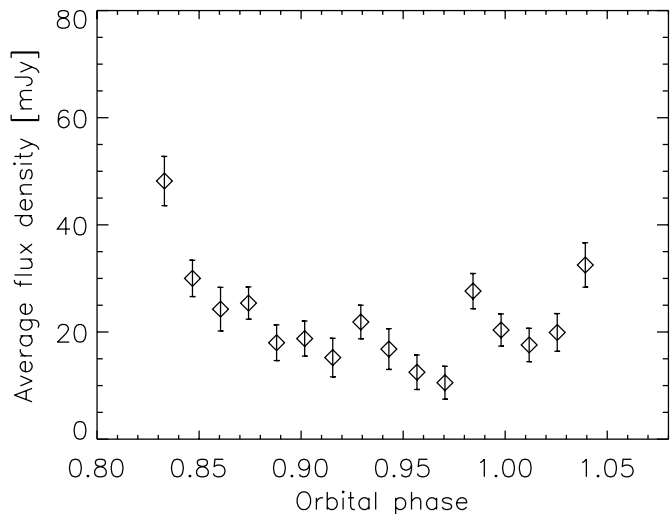


**Fig. 6.** Flux density in the 2.4–12  $\mu\text{m}$  range versus Cygnus X-3 orbital phase.

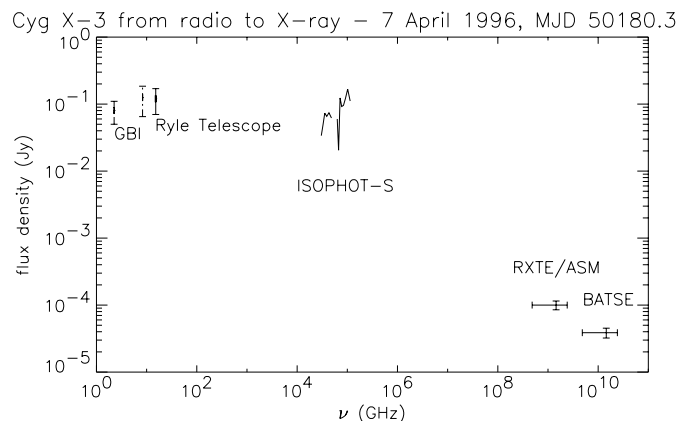
### 3.5. Radio and X-ray fluxes

Figure 7 shows the mean flux density of Cygnus X-3 on MJD 50180.3 from radio to hard X-rays. The quiescent state observed in the mid-infrared range with ISO was also seen during monitoring radio observations of Cygnus X-3 with the Ryle telescope (Mullard Radio Observatory, Cambridge) shortly before and after the ISO observations, the mean flux density at 15 GHz being about 120 mJy (Pooley 1999), and with the Green Bank Interferometer (GBI) monitoring program (McCullough et al. 1999) during a quiescent period before the ISO observations, the mean flux densities being  $80 \pm 30$  mJy at 2.25 GHz and  $125 \pm 60$  mJy at 8.3 GHz and the spectral index  $\alpha = 0.3 \pm 0.1$ . These flux densities are at least one order of magnitude higher than that observed during the quench periods of very low radio emission preceding the major flares of Cygnus X-3 (McCullough et al. 1999). In fact, this quiescent state was still present in 1996 May, June and July (Fender et al. 1999).

In the X-ray range, at the same epoch, the *Rossini XTE/All Sky Monitor* count rate was  $\sim 7.5$  counts  $\text{s}^{-1}$  corresponding to a mean flux of  $\sim 1$  mJy from 2 to 12 keV (see XTE archive and Levine et al. 1996), and the BATSE instrument on board the Compton Gamma Ray Observatory observed a mean photon flux of 0.039 count  $\text{s}^{-1}$  corresponding to a flux density of 0.04 mJy in the 20–100 keV range. Thus the mid-infrared continuum spectrum whose shape is explained by thermal free-free emission in an expanding wind has a different origin than the non-thermal radio emission and the hard X-ray emission which are closely coupled (Mioduszewski et al. 2001; Choudhury et al. 2002).

## 4. Conclusions

We have shown that the mid-infrared continuum (between 2.4–12  $\mu\text{m}$ ) of Cygnus X-3 in quiescence can be explained by the free-free emission of an expanding wind in the intermediate case between optically thick and optically thin regimes.



**Fig. 7.** Quasi-simultaneous observations of Cygnus X-3 in the radio, infrared, soft and hard X-rays on April 7, 1996, averaged over the orbital phase; the ISOPHOT-S spectrum is dereddened with the Lutz et al. (1996) law and rebinned to the resolution of 0.3  $\mu\text{m}$ ; note that the GBI was dormant after 1996 April 1 till November 1996, and that the given flux densities (in dash lines) are mean values during the quiescent period March 17 to April 1, 1996.

The low quiescent luminosity of the object in the mid-infrared allows only detection of an upper limit of 15 percent on the possible 4.8 h orbital modulation. A line at 4.3  $\mu\text{m}$  is detected at a confidence level of more than  $4.3\sigma$ , and is interpreted as the expected He I (3p–3s) emission line. The close match between the mid-infrared brightness and spectral energy distribution of Cygnus X-3 in quiescence, the He I emission line, the high mass loss rate in the wind and that of the colliding-wind Wolf-Rayet system WR 147, is consistent with a Wolf-Rayet like companion of WN8 type to the compact object in Cygnus X-3, a later type than suggested by previous works (van Kerkwijk et al. 1996; Fender et al. 1999; Hanson et al. 2000).

*Acknowledgements.* We warmly thank the ISO project and the ISOCAM and ISOPHOT Teams in Villafraanca, Saclay and Heidelberg. We express our gratitude to R. Ogley and to R. Fender for helpful comments, to G. Pooley for giving us the Ryle telescope data and to J. L. Starck for very useful discussions on data analysis. We thank the referee J. Martí for helpful comments on the manuscript. This research has made use of data from the Green Bank Interferometer, a facility of the National Science Foundation operated by the NRAO in support of NASA High Energy Astrophysics programs, of data which were generated by the CGRO BATSE Instrument Team at the Marshall Space Flight Center (MSFC) using the Earth occultation technique, and of quick-look results provided by the ASM/RXTE team. P.A. acknowledges the support of a Hungarian science grant.

## References

- Abergel, A., Bernard, J. P., Boulanger, F., et al. 1996, *A&A*, 315, L329
- Acosta-Pulido, J. A., & Ábrahám, P. 2001, in *The Calibration Legacy of the ISO Mission*
- Becklin, E. E., Neugebauer, G., Hawkins, F. J., et al. 1973, *Nature*, 245, 302
- Bonnet-Bidaud, J. M., & Chardin, G. 1988, *Phys. Rep.*, 170, 326
- Cherepashchuk, A. M., & Moffat, A. F. J. 1994, *ApJ*, 424, L53

- Choudhury, M., Rao, A. R., Vadawale, S. V., Ishwara-Chandra, C. H., & Jain, A. K. 2002, *A&A*, 383, L35
- Churchwell, E., Bieging, J. H., van der Hucht, K. A., et al. 1992, *ApJ*, 393, 329
- Crowther, P. A., Hillier, D. J., & Smith, L. J. 1995a, *A&A*, 293, 403
- Crowther, P. A., Smith, L. J., & Hillier, D. J. 1995b, *A&A*, 302, 457
- Draine, B. T. 1989, in *Infrared Spectroscopy in Astronomy*, 93
- Ergma, E., & van den Heuvel, E. P. J. 1998, *A&A*, 331, L29
- Fender, R. P., Bell Burnell, S. J., Garrington, S. T., Spencer, R. E., & Pooley, G. G. 1995, *MNRAS*, 274, 633
- Fender, R. P., Bell Burnell, S. J., Williams, P. M., & Webster, A. S. 1996, *MNRAS*, 283, 798
- Fender, R. P., Hanson, M. M., & Pooley, G. G. 1999, *MNRAS*, 308, 473
- Gabriel, C., Acosta-Pulido, J., Heinrichsen, I., Morris, H., & Tai, W.-M. 1997, in *Astronomical Data Analysis Software and Systems VI*, vol. 6, ASP Conf. Ser., 125, 108
- Giacconi, R., Gorenstein, P., Gursky, H., & Waters, J. R. 1967, *ApJ*, 148, L119
- Haas, M., Müller, S. A. H., Chini, R., et al. 2000, *A&A*, 354, 453
- Hanson, M. M., Still, M. D., & Fender, R. P. 2000, *ApJ*, 541, 308
- Kessler, M. F., Steinz, J. A., Anderegg, M. E., et al. 1996, *A&A*, 315, L27
- Kitamoto, S., Mizobuchi, S., Yamashita, K., & Nakamura, H. 1992, *ApJ*, 384, 263
- Klaas, U., Krüger, H., Heinrichsen, I., & Laureijs, R. 1994, *ISOPHOT Observers Manual*, Version 3.1, ISO Science Operations Team, ESA/ESTEC, Noordwijk, The Netherlands  
<http://www.iso.vilspa.esa.es/manuals/>
- Koch-Miramond, L., Bonnet-Bidaud, J., Abraham, P., & Claret, A. 2001, in *Black Holes in Binaries and Galactic Nuclei*, ed. L. Kaper, E. P. J. van den Heuvel, & P. A. Woudt, ESO Astrophys. Symp., 137
- Levine, A. M., Bradt, H., Cui, W., et al. 1996, *ApJ*, 469, L33
- Lutz, D., Feuchtgruber, H., Genzel, R., et al. 1996, *A&A*, 315, L269
- Martí, J., Paredes, J. M., & Peracaula, M. 2000, *ApJ*, 545, 939
- Martí, J., Paredes, J. M., & Peracaula, M. 2001, *A&A*, 375, 476
- Mason, K. O., Cordova, F. A., & White, N. E. 1986, *ApJ*, 309, 700
- McCollough, M. L., Robinson, C. R., Zhang, S. N., et al. 1999, *ApJ*, 517, 951
- Mioduszewski, A. J., Hjellming, R. M., Rupen, M. P., et al. 1998, in *Radio Emission from Galactic and Extragalactic Compact Sources*, ASP Conf. Ser., 144, IAU Colloq., 164, 351
- Mioduszewski, A. J., Rupen, M. P., Hjellming, R. M., Pooley, G. G., & Waltman, E. B. 2001, *ApJ*, 553, 766
- Mitra, A. 1996, *MNRAS*, 280, 953
- Morel, T., Marchenko, S. V., Eenens, P. R. J., et al. 1999, *ApJ*, 518, 428
- Morris, P. W., van der Hucht, K. A., Crowther, P. A., et al. 2000, *A&A*, 353, 624
- Morris, P. W., van der Hucht, K. A., Willis, A. J., et al. 1999, in *Wolf-Rayet Phenomena in Massive Stars and Starburst Galaxies*, IAU Symp., 193, 77
- Ogley, R. N., Bell Burnell, S. J., & Fender, R. P. 2001, *MNRAS*, 322, 177
- Parsignault, D. R., Gursky, H., Kellogg, E. M., et al. 1972, *Nat. Phys. Sci.*
- Pittard, J. M., Stevens, I. R., Williams, P. M., et al. 2002, *A&A*, 388, 335
- Pooley, G. G. 1999, private communication
- Schmid-Burgk, J. 1982, *A&A*, 108, 169
- Skinner, S. L., Itoh, M., Nagase, F., & Zhekov, S. A. 1999, *ApJ*, 524, 394
- Starck, J. L., Abergel, A., Aussel, H., et al. 1999, *A&AS*, 134, 135
- Stevens, I. R., & Howarth, I. D. 1999, *MNRAS*, 302, 549
- van den Heuvel, E. P. J., & de Loore, C. 1973, *A&A*, 25, 387
- van der Hucht, K. A. 2001, *New Astron. Rev.*, 45, 135
- van Kerkwijk, M. H., Charles, P. A., Geballe, T. R., et al. 1992, *Nature*, 355, 703
- van Kerkwijk, M. H., Geballe, T. R., King, D. L., van der Klis, M., & van Paradijs, J. 1996, *A&A*, 314, 521
- Vanbeveren, D., de Donder, E., van Bever, J., van Rensbergen, W., & de Loore, C. 1998, *New Astron.*, 3, 443
- Williams, P. M., Dougherty, S. M., Davis, R. J., et al. 1997, *MNRAS*, 289, 10
- Wright, A. E., & Barlow, M. J. 1975, *MNRAS*, 170, 41